# Quantum Limit Characterization of Signal-to-Noise Ratio using Phase-Shift Keying in Homodyne Detection

**Nagham J. Shukur**

[1] *Branch of Materials Science, School of Applied Sciences, University of Technology, Baghdad, Iraq*

***In this work, a mathematical treatment for the quantum limit of signal-to-noise ratio (SNR) in homodyne coherent detection was presented. This treatment is based on the case of balanced detection when the incident signal power is much lesser than the local oscillator power when the efficient AC coupling is assumed. The final results were obtained from an analytical expression of SNR dependent of the average number of incident photons and the quantum efficiency.***

***Keywords***: Phase-shift keying, DPSK, Homodyne detection, SNR, Balanced detection
**Received**: 15 December 2009, **Revised**: 24 March 2010, **Accepted**: 31 March 2010

## 1. Introduction

Although coherent detection is relatively new in optical communications, it has been around in radio communications for a long time. In both radio and optical communications, the essence of coherent detection is to generate a product term of the received signal and a local carrier. As a result, the received passband signal can be demodulated or shifted back to baseband. As an example, consider a passband signal $m(t)\cos(\omega_{inc}t)$ shown in Fig. (1a) [1].

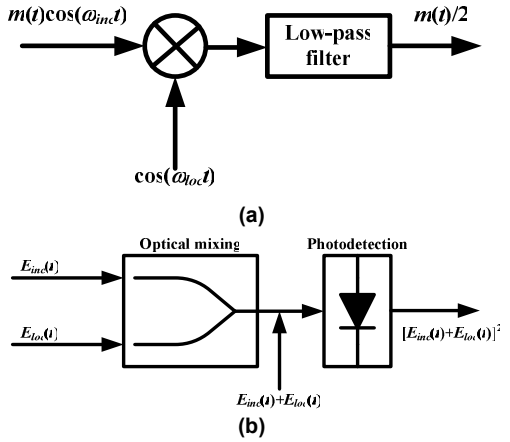


**Fig. (1) Coherent detection in (a) radio communications and (b) optical communications [1]**

To recover the original baseband signal $m(t)$, the received signal is multiplied by a local oscillator $\cos(\omega_{loc}t)$. If the local carrier is synchronized to the received signal $m(t)\cos(\omega_{inc})$ in frequency, i.e., $\omega_{inc}=\omega_{loc}$, the product term is [2]

$$m(t)\cos(\omega_{inc}t)\times\cos(\omega_{loc}t) = \frac{1}{2}m(t)+\frac{1}{2}m(t)\cos(2\omega_{inc}t) \quad (1)$$

Therefore, the baseband signal can be recovered using the low-pass filter. The above mentioned scheme is called ***homodyning*** because $\omega_{inc}=\omega_{loc}$.

Both phase-shift keying (PSK) and differential phase-shift keying (DPSK) use signal constellations consisting of number of points equally spaced on a circle. While PSK encodes each block of logarithmic number of points (bits) in the phase of the transmitted symbol, DPSK encodes each block of the same logarithmic number of points (bits) in the phase change between successively transmitted symbols [3]. Tonguz and Wagner [4] showed that the performance of DPSK with optical amplification and interferometric detection is equivalent to standard differentially coherent detection [5].

Although the use of the multiplier to generate the product term is common in radio communications, it is not practical in optical communications [6]. An alternative way is to mix the incident signal with a local optical carrier. As illustrated in Fig. (1b), if the two signals have the same polarizations, the magnitudes of their fields can be scalar added. In this case, because the photocurrent output is proportional to the combined intensity,

$$I_{ph} = R\left\{P_{inc} + P_{loc} + 2\sqrt{P_{inc}P_{loc}}\cos\left(\omega_{inc}t - \omega_{loc}t\right)\right\} \quad (2)$$

  

where $R$ is the responsivity of the photodiode and $P_{loc}$ is the local oscillator power

Among three terms, $P_{loc}$ is a constant term that can be simply filtered out by AC-coupling. The third term is the product term of interest. Because $P_{loc}>>P_{inc}$, $(P_{inc}P_{loc})^{1/2}$ is much larger than $P_{inc}$. Therefore, the latter term can be dropped.

A detailed block diagram of coherent homodyne detection is shown in Fig. (2). in homodyne detection, the carrier recovery loop uses a photodetector output to drive the carrier loop. The photodetector output carries the phase difference information of the signal and the local oscillator [1].

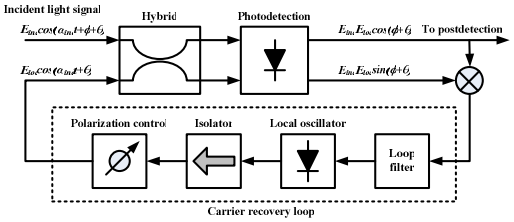


**Fig. (2) Block diagram of homodyne coherent detection**

## 2. Mathematical Treatment

Hybrid is a four-port device that mixes two light signals and, in general, its two inputs and two outputs are related by a 2x2 matrix as [7]:

$$\begin{bmatrix} E_{o1} \\ E_{o2} \end{bmatrix} = \begin{bmatrix} T_1 & X_1 \\ X_2 & T_2 \end{bmatrix} \begin{bmatrix} E_{inc} \\ E_{loc} \end{bmatrix} = \overline{H} \begin{bmatrix} E_{inc} \\ E_{loc} \end{bmatrix} \tag{3}$$

In coherent detection, there are two important types of hybrids that deserve further consideration. The first type is called the 180° hybrid, with the transfer matrix given by [1]:

$$\overline{H}_{180} = \frac{1}{\sqrt{2}} e^{i\theta} \begin{bmatrix} 1 & 1 \\ 1 & -1 \end{bmatrix} \tag{4}$$

There is a 180° phase shift between $T_1$ and $T_2$, and the hybrid is lossless because of

$|T_1|^2 + |X_2|^2 = |T_2|^2 + |X_1|^2 = 1$

The other important type of hybrid has a transfer matrix given by

$$\overline{H}_{90} = \frac{a}{\sqrt{2}} e^{j\theta} \begin{bmatrix} 1 & 1 \\ 1 & j \end{bmatrix} \tag{5}$$

where 0<a<1 is a certain loss factor from practical implementation

This hybrid is called the 90° hybrid because there is a 90° phase shift between $T_1$ and $T_2$. In practical 90° four-port hybrid design, the loss factor ($a$) cannot be greater than 0.7071 because of the limitation of physics. This implies at least a 3dB power loss and is undesirable [1,8].

After the two light signals are mixed by the hybrid, there are two main configurations used in photodetection: single detection and balanced detection, which is illustrated in Fig. (3). Single detection uses only one photodiode and this is the same as in incoherent detection. In this case, one of the hybrid's outputs is not used and can be used for carrier recovery. Balanced detection feeds the two outputs to two photodiodes whose current outputs are subtracted. One major advantage of balanced detection is that it cancels the relative intensity noise (RIN) from the local oscillator [9].

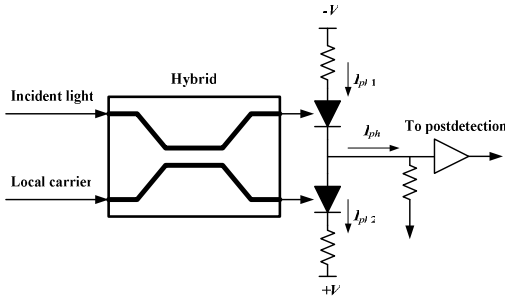


**Fig. (3) Balanced detection**

Consider the use of a 180° hybrid, the two outputs from the hybrid can thus be expressed as

$$E_{o1} = \frac{1}{\sqrt{2}}\left(E_{inc} + E_{loc}\right) \tag{6a}$$

$$E_{o2} = \frac{1}{\sqrt{2}}\left(E_{inc} - E_{loc}\right) \tag{6b}$$

After photodetection,

$$I_{ph,1} = \frac{R}{2}\left\{P_{inc} + P_{loc} + 2\sqrt{P_{inc}P_{loc}}\cos\left[\left(\omega_{inc} - \omega_{loc}\right)t + \phi(t)\right]\right\} \tag{7a}$$

$$I_{ph,2} = \frac{R}{2}\left\{P_{inc} + P_{loc} - 2\sqrt{P_{inc}P_{loc}}\cos\left[\left(\omega_{inc} - \omega_{loc}\right)t + \phi(t)\right]\right\} \tag{7b}$$

where $P_{inc}$ is the incident light power and $P_{loc}$ is the local carrier power

In amplitude modulation, $P_{inc}$ is modulated according to the transmitted data. Also, $\phi(t)$ is the phase of the carrier and can be used for phase modulation [1,10]. With balanced detection, the difference between the photocurrents is

$$\begin{aligned} I_{ph} &= I_{ph,1} - I_{ph,2} \\ &= 2R\sqrt{P_{inc}P_{loc}}\cos\left[\left(\omega_{inc} - \omega_{loc}\right)t + \phi(t)\right] \end{aligned} \tag{8}$$

This subtracted current has no DC terms and is twice that of the individual photodiode output. Therefore, use of single detection has a 3dB (factor 1/2) power loss compared to balanced detection.

### 3. Results and Discussion

Based on the balanced detection, when homodyne detection is used or $\omega_s=\omega_{loc}$, then

$$I_{ph} = 2R\sqrt{P_{inc}P_{loc}}\cos[\phi(t)] \quad (9)$$

In the case of homodyne detection, the photocurrent signal given by Eq. (9) is a baseband signal and immediately ready for detection. Specifically, as shown in Fig. (4), the photocurrent output from homodyne detection is first equalized by a matched filter and then followed by threshold detection. When the shot noise is approximated as Gaussian and there is no inter-symbol interference (ISI), this match filtering structure gives the optimum detection performance. When the input pulse is rectangular or a non-return-to-zero (NRZ) pulse, the matched filtering is equivalent to integrate-and-dump [11].

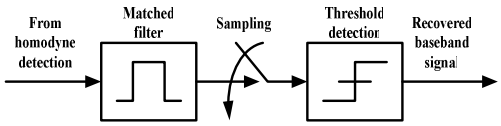


**Fig. (4) Postdetection for homodyne detection**

The current outputs given in Eqs. (7a) and (7b) contain only signal terms. In practice, there are additional noise terms that need to be added. In addition to receiver noise, two important noise terms are the shot noise from photodetection and the RIN from the local oscillator. Because the RIN power is proportional to the local optical power, which is much larger than the received signal power, the RIN can greatly affect detection performance. When balanced detection is used, the same RIN occurs at the two photodiode outputs. Therefore, by subtracting the two current outputs from balanced detection, the RIN can be cancelled [4,12].

After the RIN is cancelled, the only noise term to consider the shot noise because of the high local optical power. The two-sided power spectral density (PSD) of noise at each photodiode output is [1]

$$S_{n,i}(\omega) = \frac{1}{2}qRP_{loc} \quad (10)$$

where $i$ is either 1 or 2

When the two current outputs are subtracted in balanced detection, the total noise power is

$$S_{n,i}(\omega) = S_{n,1}(\omega) + S_{n,2}(\omega) = qRP_{loc}B \quad (11)$$

Shot noise can be assumed to be Gaussian when the noise power is large [13-14]. If an integrate-and-dump filter is used in Fig. (15.6) as the matched filter for homodyne detection, the noise power at the threshold detector input is

$$\sigma_n^2 = qRP_{loc}T \quad (12)$$

From Eqs. (9) and (12), the signal-to-noise ratio (SNR) in homodyne detection is given by

$$SNR = \frac{\left(2R\sqrt{P_{inc}P_{loc}}T\right)^2}{qRP_{loc}T} = \frac{4\eta P_{inc}T}{hf} = 4\eta N \quad (13)$$

where $N$ is the average number of incident photons over the period $T$, $\eta$ is the quantum efficiency, and $R=q\eta/hf$

A SNR of 36 is needed to achieve a bit error rate (BER) of $10^{-9}$ for phase-shift keying (PSK) ($\phi$=0 or $\pi$ in Eq. (9)). If $\eta$=1, $N$ must equal ($P_{inc}T/hf$)=9 photons per bit, which is the quantum limit using PSK homodyne detection [15].

As shown in Fig. (5), signal-to-noise ratio (SNR) is varying with the incident signal power ($P_{inc}$) at different responsivities. It is clear that the higher responsivity dump the noise to very small levels (negligible) as the incident signal power is increased with assumption of constant local oscillator power ($P_{loc}$).

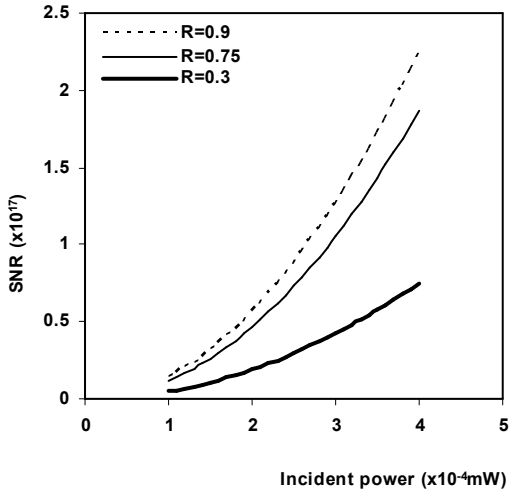


**Fig. (5) Variation of SNR with incident power ($P_{inc}$) at different responsivities**

Figure (6) shows that the shorter period taken by the incident photons to reach the detecting element is leading to undesirable levels of noise within the whole detection system. Therefore, it is important to control this period in order to prevent the noise from dominate the output signal or at least to limit the noise at rather acceptable levels not affecting the bit rate toward decrease. However, operating at very long periods may cause to stimulate some other types of noise those are not desirable at all in such detection systems [16].

It seems that there is no limit for increasing the number of incident photons per bit versus SNR, as shown in Fig. (7), at the low rates (<100photons/bit) as these photons are contributing to the output signal with low noise level. However, SNR does not reach very high levels despite the further increasing in the number of incident photons per bit because of the output signal saturation, which is an important

  

limitation in such optoelectronic devices and systems.

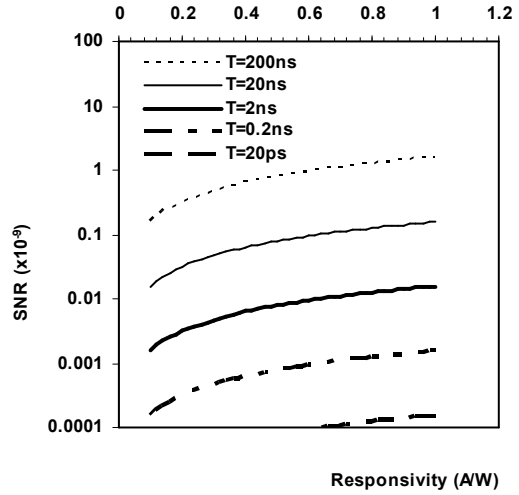


**Fig. (6) Variation of SNR with responsivity (*R*) at different periods**

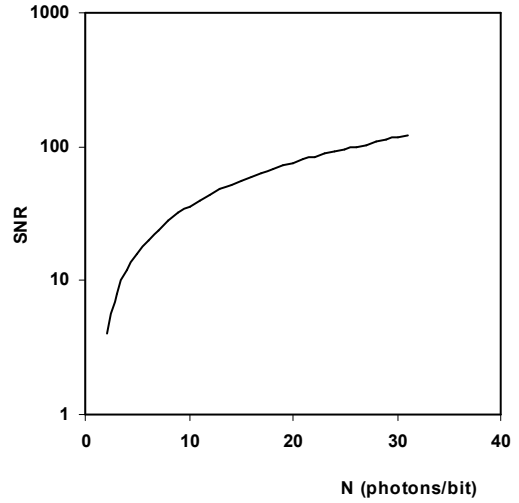


**Fig. (7) Variation of SNR with number of incident photons (*N*)**

## 4. Conclusion

From the results obtained in this work, the quantum limit of signal-to-noise ratio (SNR) in homodyne coherent detection was introduced. The behavior of SNR as a function of several parameters, such as incident signal power, responsivity and number of incident photons per bit, was explained for the case of balanced detection when the incident signal power is much lesser than the local oscillator power ($P_{loc}>>P_{inc}$) with the assumption of efficient AC coupling. In conclusion, the SNR can be expressed in terms of number of incident photons per bit and the quantum efficiency for an acceptable level as $4\eta N$.

## References

[1] M.M.-K. Liu, **"Principles and Applications of Optical Communications"**, McGraw-Hill Co., Inc. (Chicago, U.S.A) (1996), Ch. 15, 754-770.

[2] A.R. Chraplyvy, *IEEE J. of Lightwave Technol.*, 8(10) (1990) 1548-1557.

[3] O.K. Tonguz and R.E. Wagner, *IEEE Photon. Technol. Lett.*, 3 (1991) 835-837.

[4] J.G. Proakis, **"Digital Communications"**, 4th ed., McGraw-Hill (2000).

[5] D.M. Kuchta and C.J. Mahon, *IEEE Photon. Technol. Lett.*, 6(2) (1994) 288-290.

[6] D. Marcuse, *IEEE J. of Lightwave Technol.*, 9(4) (1991) 505-513.

[7] S. Walklin and J. Conradi, *J. of Lightwave Technol.*, 17 (1999) 2235–2248.

[8] J. Wang and J.M. Kahn, *J. Lightwave Technol.*, 22(2) (2004) 362–371.

[9] P.S. Henry, "Error-rate performance of optical amplifiers", *Proc. of Conf. on Optical Fiber Commun.*, Washington, DC, 1989, p. 170.

[10] P.A. Humblet and M. Azizoglu, *J. Lightwave Technol.*, 9 (1991) 1576–1582.

[11] J. Rebola and A. Cartaxo, *Proc. of SPIE*, 4087 (2000) 49–59.

[12] B. Jorgensen, B. Mikkelsen and C. Mahon, *J. Lightwave Technol.*, 10 (1992) 660–671.

[13] C.P. Kaiser, P.J. Smith and M. Shafi, *J. Lightwave Technol.*, 13 (1995) 525–533.

[14] S. Norimatsu and K. Iwashita, *J. Lightwave Technol.*, 10 (1992) 341–349.

[15] J.R. Barry and J.M. Kahn, *J. Lightwave Technol.*, 10 (1992) 1939–1951.

[16] J.D. Berger, Y. Zhang, J.D. Grade, H. Lee, S. Hrinya, H. Jerman, A. Fennema, A. Tselikov, and D. Anthon, "Widely tunable external cavity diode laser using a MEMS electrostatic rotary actuator", Proc. of 27th Euro. Conf. on Optical Commun. Amsterdam, Netherlands, Sept. 30-Oct. 4, 2001.